



COMPEL  
26,2

452

Received September 2005  
 Revised October 2006  
 Accepted October 2006

## OTHER ARTICLE

# VHDL-AMS based genetic optimisation of fuzzy logic controllers

L. Wang and T.J. Kazmierski  
*School of Electronics and Computer Science,  
 University of Southampton, Southampton, UK*

### Abstract

**Purpose** – This paper presents a VHDL-AMS based genetic optimisation methodology for fuzzy logic controllers (FLCs) used in complex automotive systems and modelled in mixed physical domains. A case study applying this novel method to an active suspension system has been investigated to obtain a new type of fuzzy logic membership function with irregular shapes optimised for best performance.

**Design/methodology/approach** – The geometrical shapes of the fuzzy logic membership functions are irregular and optimised using a genetic algorithm (GA). In this optimisation technique, VHDL-AMS is used not only for the modelling and simulation of the FLC and its underlying active suspension system but also for the implementation of a parallel GA directly in the system testbench.

**Findings** – Simulation results show that the proposed FLC has superior performance in all test cases to that of existing FLCs that use regular-shape, triangular or trapezoidal membership functions.

**Research limitations** – The test of the FLC has only been done in the simulation stage, no physical prototype has been made.

**Originality/value** – This paper proposes a novel way of improving the FLC's performance and a new application area for VHDL-AMS.

**Keywords** Fuzzy logic, Genetics, Algorithmic languages

**Paper type** Research paper

### Introduction

This paper presents a general approach to complex hardware system optimisation using a hardware description language (HDL). Traditionally, hardware systems are optimised using a dedicated software application which invokes a suitable HDL simulator (Hounsell and Arslan, 2000). This dedicated software for optimisation, called the optimiser, needs to send parameters to the HDL simulator, start simulation, get back the simulation results and do the evaluation repeatedly. The interaction between the optimiser and the simulator normally requires multiple data transfers and may lead to program collision. It has been reported that the integration of optimization and simulation has become nearly ubiquitous in practice (Fu *et al.*, 2000). The salient feature of the technique presented here is that the hardware description testbench includes a GA optimiser which concurrently simulates multiple instances of the system (chromosomes). In this way, both the hardware system and optimiser are integrated within the HDL. Our GA optimiser is implemented in VHDL-AMS and was successfully applied to a case study where it helps to significantly improve the performance of the FLC in an AASS.



Automotive suspension systems reduce the vibrations between the sprung and unsprung masses caused by the motion of an automobile so that the vehicle's ride quality could be improved. According to the system's ability to add or extract energy, the suspension systems can be classified as passive, semi-active or active (Sam *et al.*, 2000). Passive suspension consists of conventional springs and dampers only and it cannot add energy to the system. Semi-active suspension does not add energy either but changes the damping coefficient of the shock absorbers dynamically to obtain a better suspension quality. An active suspension system contains an actuator, which can generate a force acting on the sprung and unsprung masses, as well as the springs and dampers.

The advantages of active suspension systems over passive and semi-active ones have been known for many years (Tan and Bradshaw, 1997). However, the design of a suitable active suspension controller, which determines the value of the actuator force according to the dynamic motions of the sprung and/or unsprung mass, is difficult and still attracts researchers' interest. A number of different control algorithms have been established (Alleyne and Hedrick, 1995; Yagiz *et al.*, 1997; Sam *et al.*, 2000; Chantranuwathana and Peng, 2004). Accurate performance analysis and optimisation of such systems is difficult since the input to an AASS (i.e. the road displacement) is unpredictable. Fuzzy logic controllers, due to their ability of handling uncertain and complex systems, have emerged as a promising technique for high-performance AASSs (Son and Isik, 1996; Barr and Ray, 1996; Al-Holou *et al.*, 1999). FLCs are based on the general principles of the fuzzy set theory (Zadeh, 1965) and their input and output variables are similar to those of a conventional controller. FLC designs reported so far show satisfactory suspension behaviour and use regularly-shaped, usually triangular or trapezoidal, membership functions.

A genetic algorithm is an optimisation method based on natural selection (Goldberg, 1989). It has been reported to optimise various features of a fuzzy controller. For example, a GA was used to optimise the decision-making rules for fuzzy PI/PD controllers (Kuo and Li, 1999). The input variables to an FLC can also be chosen by a GA (Hashiyama *et al.*, 1995). A GA has also been used to tune the vertices of triangular membership functions of an FLC (Moon and Kwon, 1996). In the research presented in this paper, a GA is used to optimize not only the vertices but also the geometrical shapes of the fuzzy logic membership functions to further improve an FLC's performance. A GA usually has the following elements: populations of chromosomes, selection according to fitness, crossover to produce new offspring, and random mutation of new offspring (Mitchell, 1996). The stochastic nature of GA makes it suitable for fuzzy logic applications.

VHDL-AMS is a HDL designed to support hardware modelling at various abstraction levels in mixed, electrical and non-electrical physical domains using mixed, digital and analogue components (Christen and Bakalar, 1999). It has been recommended as the unified modelling language for the automotive industry by several sources (Moser and Mittwollen, 1998; VDA/FAT Working Group AK 30, 2004). The concurrent nature of VHDL-AMS processes makes the implementation of a GA optimisation system efficient and straightforward.

### System model

Figure 1 shows a linear 2-DOF (degree of freedom) quarter-car model. It is simple but contains the basic features of active suspension, thus can be found in many published applications (Ulsoy *et al.*, 1994). The dynamic motions of the sprung and unsprung

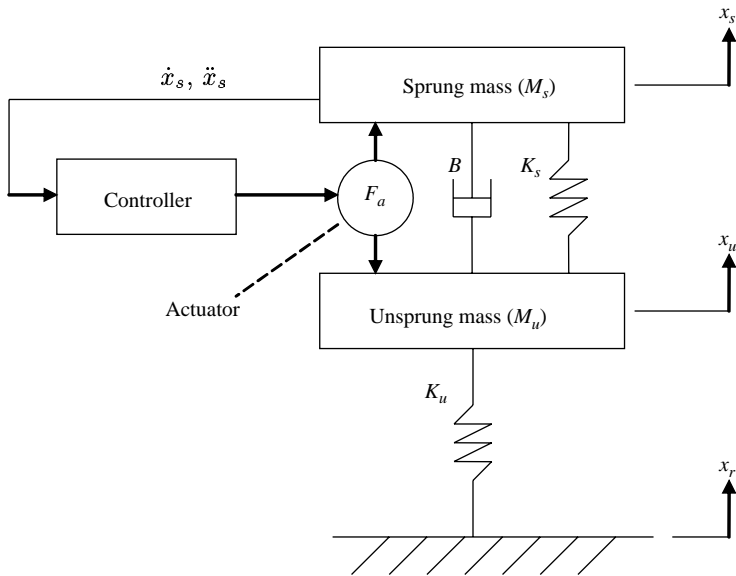


**Figure 1.**  
Active suspension system

masses are described by equations (1) and (2) (Rajamani and Hedrick, 1994) which can be obtained from Newton’s second law:

$$\ddot{x}_s M_s = K_s(x_u - x_s) + B(\dot{x}_u - \dot{x}_s) + F_\alpha \tag{1}$$

$$\ddot{x}_u M_u = -K_s(x_u - x_s) - B(\dot{x}_u - \dot{x}_s) + K_u(x_r - x_u) - F_\alpha \tag{2}$$

where  $M_s$  and  $M_u$  are vehicle’s sprung and unsprung masses,  $x_s$ ,  $x_u$  and  $x_r$  are the displacement of sprung mass, unsprung mass and road, respectively,  $K_s$  and  $B$  are the coefficients of the passive spring and damper,  $K_u$  is the tire spring rate and  $F_\alpha$  is the actuator force. The numerical values of the system parameters are listed in Table I.

The velocity  $\dot{x}_s$  and acceleration  $\ddot{x}_s$  of the automobile sprung mass  $M_s$  are chosen as the inputs to the FLC. The output is the actuator force  $F_\alpha$ . The fuzzy sets of the input and output variables are represented by three linguistic variables: positive ( $P$ ), zero ( $Z$ ) and negative ( $N$ ). With these linguistic variables, a set of nine fuzzy rules is developed, as shown in Table II. These rules were generated by using basic engineering sense. For example, if the velocity is zero and the acceleration is positive then the mass’s velocity is going to increase and a negative force should be applied.

| Symbol                 | Value         |
|------------------------|---------------|
| $M_s$                  | 250.0 kg      |
| $M_u$                  | 30.0 kg       |
| $K_s$                  | 15,000.0 N/m  |
| $B$                    | 1,000.0 N/m/s |
| $K_u$                  | 150,000.0 N/m |
| $F_\alpha, \text{max}$ | 1,500.0 N     |

**Table I.**  
Numerical values of  
system parameters

The fuzzy inference procedure used is the max-product composition (Sugeno, 1985). Assuming that the sprung mass velocity has the degree of membership  $v_P, v_Z$  and  $v_N$  in positive ( $P$ ), zero ( $Z$ ) and negative ( $N$ ), respectively, and the sprung mass acceleration has the degree of membership  $a_P, a_Z$  and  $a_N$ , the positive degree of the output force  $F_\alpha$  is:

$$F_P = \max(a_N * v_N, a_N * v_Z, a_Z * v_N) \tag{3}$$

Similarly, the zero and negative degree of  $F_\alpha$  are:

$$F_Z = \max(a_N * v_P, a_Z * v_Z, a_P * v_N) \tag{4}$$

$$F_N = F_a \max(a_P * v_P, a_Z * v_P, a_P * v_Z) \tag{5}$$

The defuzzification method employed is the centre of gravity approach (Barr and Ray, 1996). The output force is calculated as:

$$F_\alpha = \frac{F_\alpha \max * (F_P - F_N)}{F_P + F_Z + F_N} \tag{6}$$

**Shape optimisation of membership functions**

In fuzzy logic theory, a membership function is a graphical representation of the input’s degree of participation in a fuzzy set. The geometrical shapes of the membership functions used can seriously affect the performance of an FLC. For example, although triangular membership functions are very basic and widely used in active suspension controllers (Son and Isik, 1996; Al-Holou *et al.*, 1999), it was also illustrated that trapezoidal membership functions may generate superior results in certain applications (Barr and Ray, 1996) (Figure 2).

Here, we investigate the possibility of using irregular shapes of the FLC membership functions. This adds more DOF to the FLC and more scope for performance optimisation. In a specific application, such irregular shapes can be calculated by optimisation to enhance the system’s performance (Figure 3). Irregular membership functions are unlikely to lead to more complex hardware implementations given the fact that electronic control units are quite common in today’s automobile design.

In the GA optimisation, instances of the AASS, including the FLC, are invoked and each instance of the system represents a chromosome. Since, the centre of gravity method is used for defuzzification, it is only necessary to optimise the membership functions of the input variables.

For each of the two input variables,  $N$  points from the positive curve and  $N$  points from the right half of the zero curve are selected as genes. This is because a

|          |   | Acceleration |   |   |
|----------|---|--------------|---|---|
| Velocity | P | P            | Z | N |
|          | Z | N            | N | Z |
|          | N | N            | Z | P |
|          |   | Z            | P | P |

**Table II.**  
Fuzzy rules base

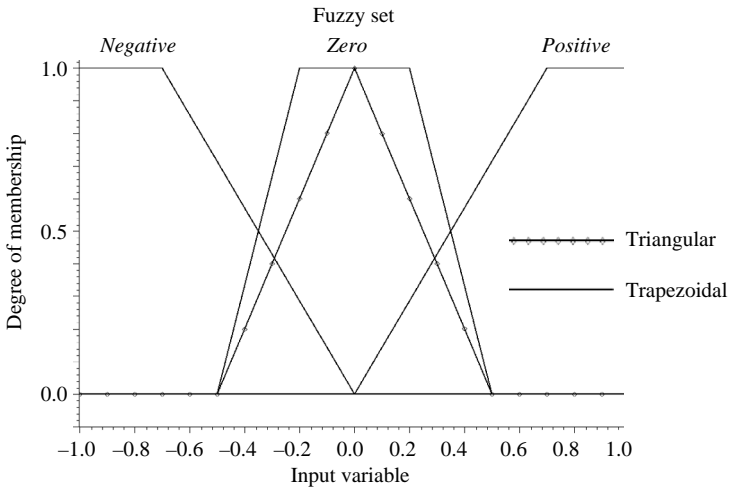


**Figure 2.**  
Fuzzy logic triangular and trapezoidal membership functions

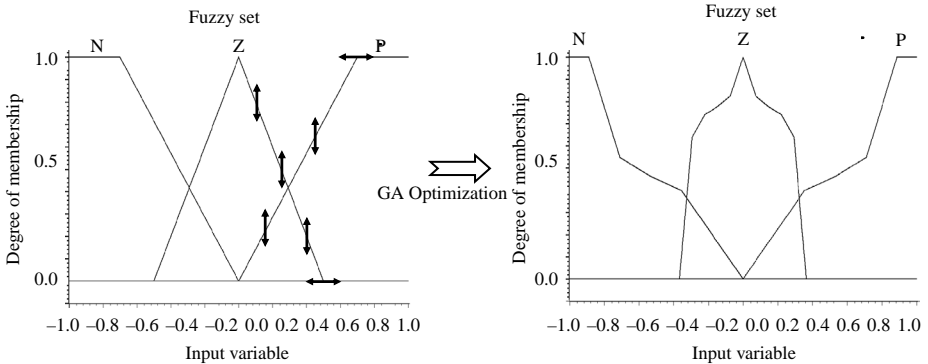


**Figure 3.**  
Optimisation of the shapes of fuzzy logic membership functions

membership function is typically symmetrical about the  $y$ -axis. These points are equally distributed along the  $x$ -axis and their  $y$ -values can be adjusted between 0 and 1. The points are simply connected by straight lines to form piecewise linear membership functions. Improving the ride comfort of an AASS means reducing the sprung mass acceleration (Chantranuwathana and Peng, 2004). So the optimisation goal is to minimize the peak-to-peak value of the sprung mass acceleration  $a_s(\ddot{x}_s)$  when the system is subject to some kind of stimulus.

**Parallel GA in VHDL-AMS testbench**

In the VHDL-AMS implementation, the chromosome is modelled as a component with  $4N$  genes as input parameters, the road displacement  $x_r$  as the excitation and the peak-to-peak value  $a_{pp}$  as the output fitness. Since,  $a_{pp}$  is a value over a certain time period, a process is needed to track its maximum and minimum value and output the peak-to-peak value at the end. Figure 4 is the block diagram of the chromosome. It shows how different components in the VHDL-AMS entity are connected.

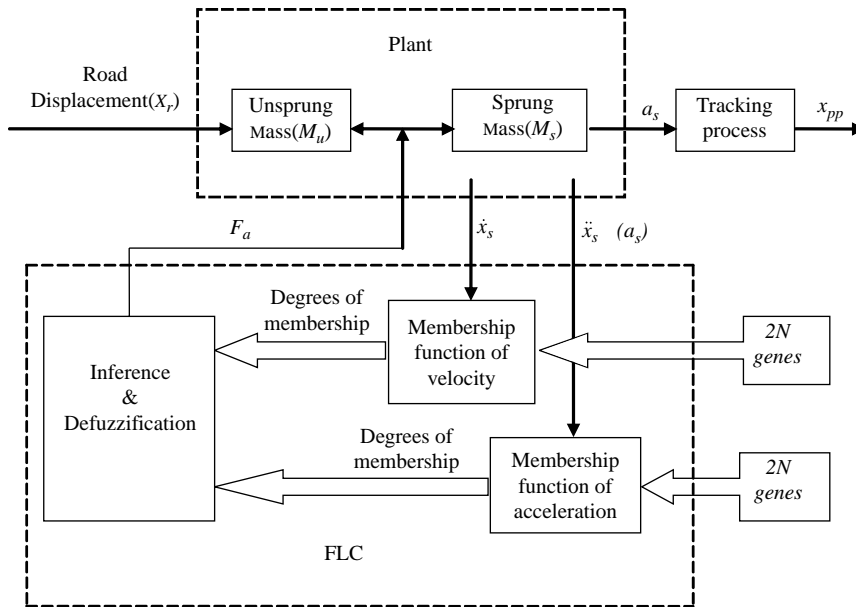


**Figure 4.**  
Block diagram of one  
chromosome

A flow chart of how the parallel GA is implemented and executed in the VHDL-AMS testbench is shown in Figure 5. Unlike most existing computer implementations of GA that evaluate one chromosome iteratively to form a population, in the VHDL-AMS based optimisation here, the chromosomes of a population are implemented in parallel. The genes are initialized by uniformly distributed random numbers. The same stimulus is applied to the population and all the chromosomes are evaluated simultaneously to get a vector of fitness values. The tournament selection is chosen as the parent selection method, because it prevents premature convergence with efficient computations (Mitchell, 1996). The selection method uses fitness values in which parents with higher fitness (i.e. smaller  $a_{pp}$ ) are more likely to be selected to produce offspring. Elitism is also used to improve GA's performance by artificially inserting the best solution into each new generation. Since, the genes are real numbers, arithmetic crossover is used to generate the offspring (Herrera *et al.*, 2003). Finally, gene mutation is employed to introduce new solutions into the new population. The evaluation-selection-crossover-mutation process is repeated until all the chromosomes converge to the same fitness. In VHDL-AMS, this loop is controlled by a finite state machine.

### Experimental results

In the GA optimisation, the number of points on each membership curve  $N$  is chosen as 5. So there are totally 20 genes in one chromosome. The population size is 100 chromosomes. The crossover and mutation rate are 0.8 and 0.01, respectively. The stimulus is a single sine-wave period jolt with added filtered Gaussian noise (GN) to reflect realistic effects of an uneven road surface. The sine-wave jolt is of a 10 cm amplitude and the period of 200 ms (5 Hz). The GN has a 1 cm standard deviation and is passed through a 50 Hz low-pass filter. The formation of the stimulus is based on

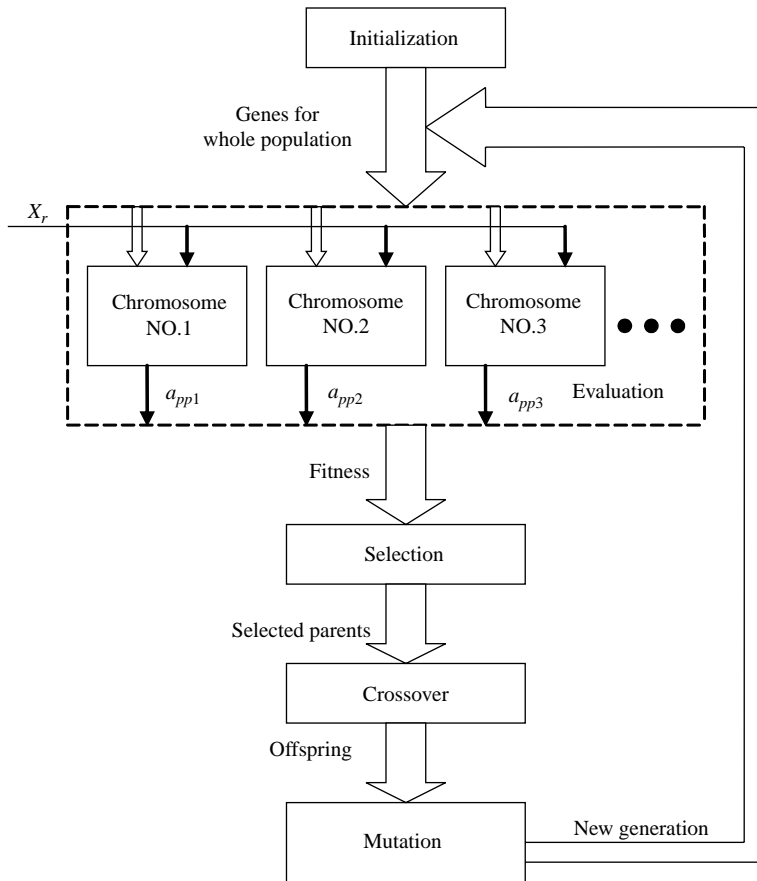


**Figure 5.**  
GA optimisation in a  
VHDL-AMS testbench  
using concurrently  
running chromosomes

two considerations. Firstly, for ride and handling characteristics the most important frequency range is 0.5-50 Hz, of which 5 Hz is the logarithmic middle-value. Anything below 0.5 Hz is too small to cause any suspension deflection, while frequencies above 50 Hz are outside the bandwidth of tyre and suspension dynamics (Truscott and Burton, 1994). Secondly, the actual road displacement inputs are of a random nature, thus some pseudo-random noises have been added. The stimulus is repeated every 4 s, which is the system's settling time. The peak-to-peak value of  $a_s(t)$ ,  $a_{pp}$ , is also updated every 4 s as a measure of the chromosome's fitness. Simulations were carried out using the SystemVision (Mentor Graphics Corporation, 2004) VHDL-AMS simulator from Mentor Graphics. After simulating the testbench for 800 s, which corresponds to 200 generations in the GA optimisation, the shapes of the membership functions converge to an optimum. The GA optimised membership function for sprung mass velocity is shown in Figure 6. The values of the genes, i.e. the locations of points on the curves, are listed in Table III. The GA optimised membership function for sprung mass acceleration is shown in Figure 7 and Table IV. The simulation CPU time was 14 h 6 min on a Pentium 4 PC.

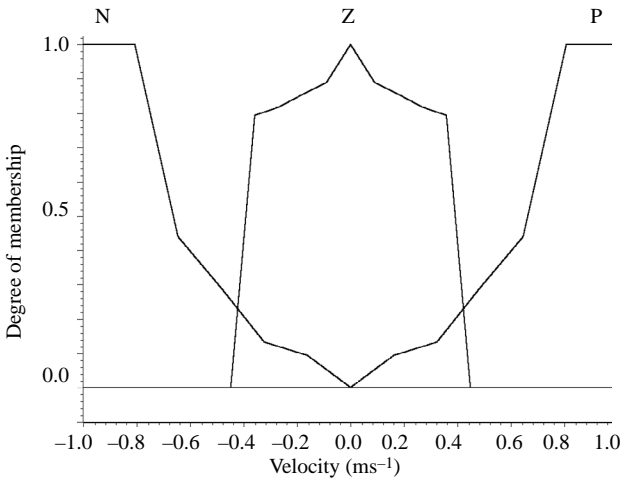


**Figure 6.**  
GA optimised  
membership function for  
sprung mass velocity

| <i>P</i> curve ( <i>x</i> , <i>y</i> ) | <i>Z</i> curve ( <i>x</i> , <i>y</i> ) |
|----------------------------------------|----------------------------------------|
| 0.0, 0.0                               | 0.0, 1.0                               |
| 0.16148, 0.09362                       | 0.08967, 0.88967                       |
| 0.32297, 0.13214                       | 0.17934, 0.85452                       |
| 0.48444, 0.29025                       | 0.26902, 0.81742                       |
| 0.64594, 0.43974                       | 0.35869, 0.79367                       |
| 0.80742, 1.0                           | 0.44836, 0.0                           |

**Table III.**  
Location of the points on  
the *P* and *Z* curves of  
velocity membership  
function

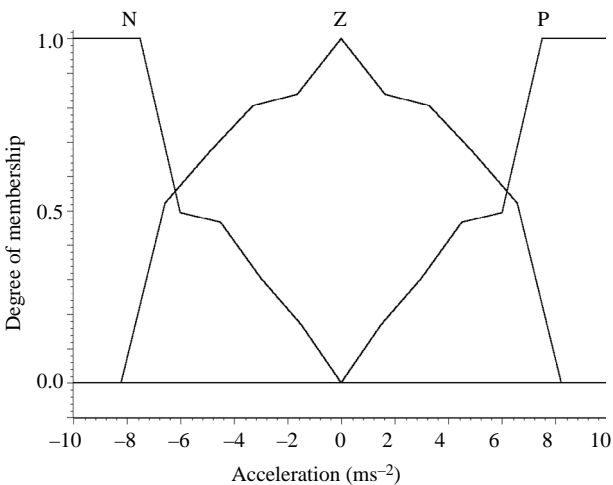


**Figure 7.**  
GA optimised  
membership function for  
sprung mass acceleration



COMPEL  
26,2

Table V lists the fitness value of the best chromosome every 25 generations. Because elitism is employed, the GA optimisation converges quickly.

Then, the GA-optimised membership functions are implemented in the FLC and simulated. For comparison, the passive suspension system and the FLCs using triangular and trapezoidal membership functions (Figure 8) are also investigated.

460

**Table IV.**  
Location of the points on the *P* and *Z* curves of acceleration membership function

| <i>P</i> curve ( <i>x</i> , <i>y</i> ) | <i>Z</i> curve ( <i>x</i> , <i>y</i> ) |
|----------------------------------------|----------------------------------------|
| 0.0, 0.0                               | 0.0, 1.0                               |
| 1.5017, 0.16972                        | 1.6440, 0.83747                        |
| 3.0035, 0.30431                        | 3.2880, 0.80447                        |
| 4.5052, 0.46677                        | 4.9321, 0.66847                        |
| 6.0070, 0.49343                        | 6.5761, 0.52093                        |
| 7.5087, 1.0                            | 8.2201, 0.0                            |

**Table V.**  
Convergence process of  $a_{pp}$

| Generation no. | 1     | 25    | 50    | 75    | 100   | 125   | 150   | 175   | 200   |
|----------------|-------|-------|-------|-------|-------|-------|-------|-------|-------|
| Fitness value  | 55.31 | 50.90 | 50.04 | 49.91 | 49.88 | 49.54 | 48.79 | 48.79 | 48.79 |

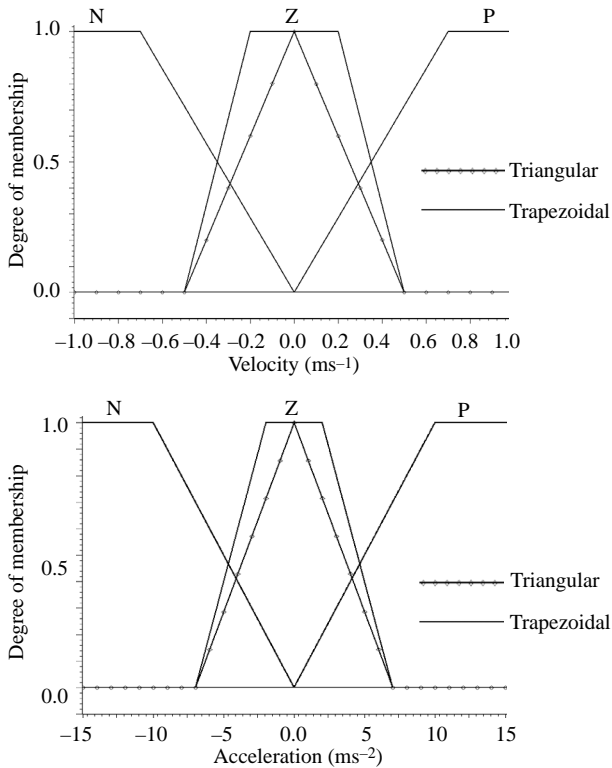


**Figure 8.**  
Triangular and trapezoidal membership functions

Four types of road displacement  $x_r$  have been used as system inputs. Simulation results of the four test cases are shown below.

*Case 1: Sine-wave jolt with Gaussian noise.* In this test case,  $x_r$  is the same as the stimulus used in the GA optimisation, a single 5 Hz sine-wave jolt with low-pass-filtered GN. The simulation waveforms of the passive suspension and three types of FLCs are shown in Figure 9. Table VI lists the peak-to-peak values of  $a_s(a_{pp})$  and the RMS (root mean square) values of  $a_s$ . The conventional FLCs can reduce  $a_{pp}$  from 57.6 to 54.0  $\text{ms}^{-2}$  (triangular) and 53.4  $\text{ms}^{-2}$  (trapezoidal). The GA-optimized FLC developed here can further decrease the value to 48.8  $\text{ms}^{-2}$ . In the following test cases, the GA optimised FLC is subjected to different types of stimulus to test the generalisation performance of the GA optimisation.

*Case 2: 5 Hz sine-wave jolt.* The second  $x_r$  is a single 5 Hz sine-wave jolt of a 10 cm amplitude, which is of the same frequency as the stimulus used for optimisation but without added noise.

Simulation results are shown in Figure 10 and Table VII.

*Case 3: 2.5 Hz sine-wave jolt.* Here,  $x_r$  is a single 2.5 Hz sine-wave jolt of a 10 cm amplitude.

The frequency is different from the stimulus used for optimisation. Simulation results are shown in Figure 11 and Table VIII.

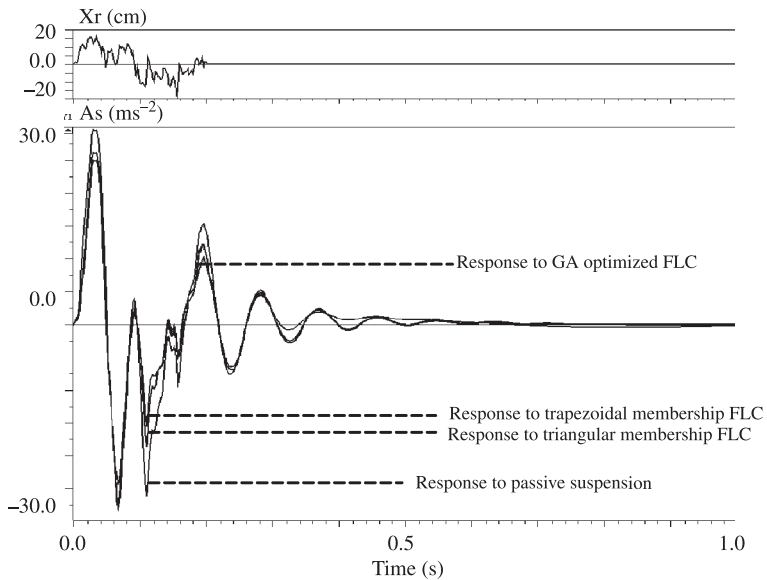


**Figure 9.**  
Waveforms for noisy jolt  
excitation (case 1)

| FLC type           | $a_{pp}$ ( $\text{ms}^{-2}$ ) | RMS of $a_s$ ( $\text{ms}^{-2}$ ) |
|--------------------|-------------------------------|-----------------------------------|
| Passive suspension | 57.569                        | 4.3997                            |
| Trapezoidal        | 53.420                        | 3.6398                            |
| Triangular         | 54.043                        | 3.6589                            |
| GA optimised       | 48.794                        | 3.3711                            |

**Table VI.**  
Peak-to-peak and RMS  
values of responses to  
noisy jolt excitation  
(case 1)

COMPEL  
26,2

462

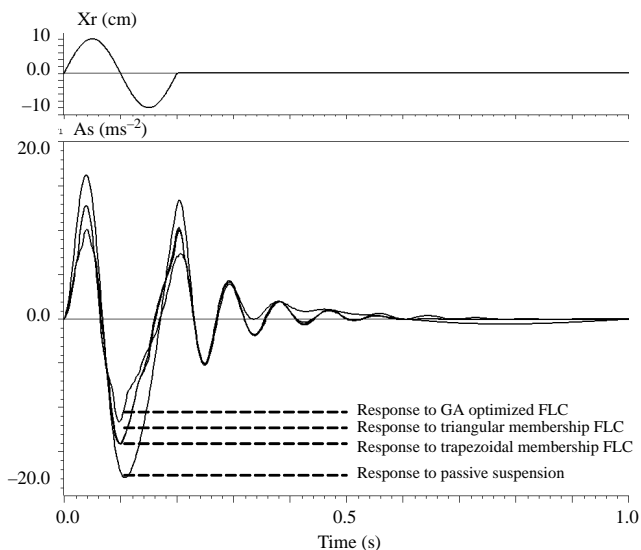


**Figure 10.**  
Waveforms for 5 Hz  
sine-wave jolt excitation  
(case 2)

| FLC type           | $a_{pp}$ ( $ms^{-2}$ ) | RMS of $a_s$ ( $ms^{-2}$ ) |
|--------------------|------------------------|----------------------------|
| Passive suspension | 34.150                 | 3.4927                     |
| Trapezoidal        | 26.924                 | 2.5281                     |
| Triangular         | 26.868                 | 2.5384                     |
| GA optimised       | 21.743                 | 2.0461                     |

**Table VII.**  
Peak-to-peak and RMS  
values of responses to  
5 Hz sine-wave jolt  
excitation (case 2)

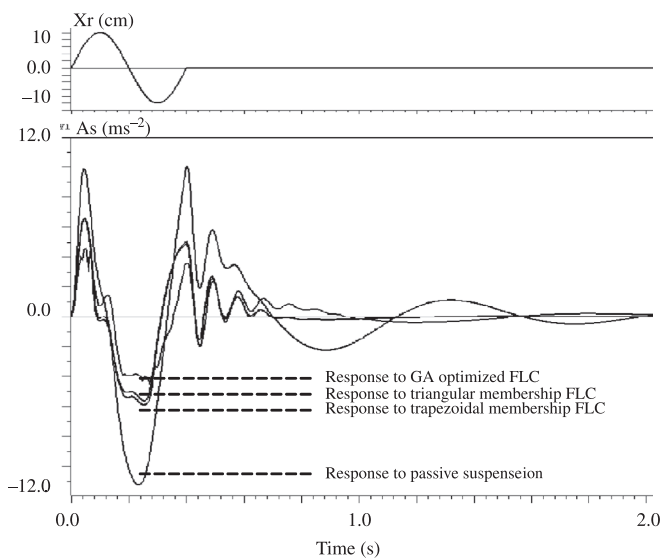


**Figure 11.**  
Waveforms for 2.5 Hz  
sine-wave jolt excitation  
(case 3)

*Case 4: Trapezoidal bump.* The  $x_r$  is of a different shape from the stimulus used for optimisation. The trapezoidal bump has the amplitude of 10 cm and lasts for 200 ms. Simulation results are shown in Figure 12 and Table IX.

In all the above test cases, the GA-optimised FLC shows improvements in both the peak-to-peak and RMS values of sprung mass acceleration to that of FLCs using trapezoidal and triangular membership functions. The results demonstrate that the proposed optimisation method has good generalisation performance.

**Conclusion**

This paper proposes a novel approach to complex hardware system optimisation in which the optimiser is a part of the HDL-based simulation testbench. A VHDL-AMS

| FLC type           | $a_{pp}$ ( $ms^{-2}$ ) | RMS of $a_s$ ( $ms^{-2}$ ) |
|--------------------|------------------------|----------------------------|
| Passive suspension | 21.338                 | 3.2440                     |
| Trapezoidal        | 12.494                 | 1.7410                     |
| Triangular         | 12.164                 | 1.6621                     |
| GA optimised       | 9.0098                 | 1.2997                     |

**Table VIII.** Peak-to-peak and RMS values of responses to 2.5 Hz sine-wave jolt excitation (case 3)

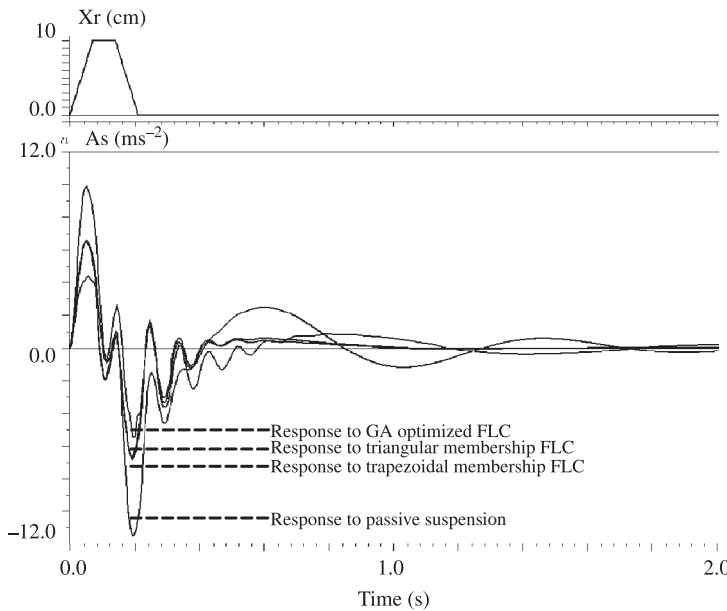


**Figure 12.** Waveforms for trapezoidal bump excitation (case 4)

| FLC type           | $a_{pp}$ ( $ms^{-2}$ ) | RMS of $a_s$ ( $ms^{-2}$ ) |
|--------------------|------------------------|----------------------------|
| Passive suspension | 21.340                 | 2.3455                     |
| Trapezoidal        | 13.355                 | 1.3458                     |
| Triangular         | 13.207                 | 1.2929                     |
| GA optimised       | 9.8305                 | 1.1336                     |

**Table IX.** Peak-to-peak and RMS values of responses to trapezoidal bump excitation (case 4)

implementation of a parallel GA was successfully used to optimise the shapes of fuzzy logic membership functions to improve the performance of the fuzzy logic controller in an automotive active suspension system. The simulation results show that the GA-optimised fuzzy logic controller with irregular membership function shapes shows superior performance to that of conventional controllers with triangular or trapezoidal membership functions.

### References

- Al-Holou, N., Weaver, J., Lahdhiri, T. and Joo, D.S. (1999), "Sliding mode-based fuzzy logic controller for a vehicle suspension system", *Proceedings on American Control Conference*, pp. 4188-92.
- Alleyne, A. and Hedrick, J. (1995), "Nonlinear adaptive control of active suspensions", *IEEE Transactions on Control Systems Technology*, Vol. 3 No. 1, pp. 94-101.
- Barr, A. and Ray, J. (1996), "Control of an active suspension using fuzzy logic", *Proceedings of the Fifth IEEE International Conference on Fuzzy Systems*, pp. 42-8.
- Chantranuwathana, S. and Peng, H. (2004), "Adaptive robust force control for vehicle active suspensions", *International Journal of Adaptive Control and Signal Processing*, Vol. 18 No. 2, pp. 83-102.
- Christen, E. and Bakalar, K. (1999), "VHDL-AMS – a hardware description language for analog and mixed-signal applications", *IEEE Transactions on Circuits and Systems II: Analog and Digital Signal Processing*, Vol. 46, pp. 1263-72.
- Fu, M., Andradottir, S., Carson, J., Glover, F., Harrell, C., Ho, Y.-C., Kelly, J. and Robinson, S. (2000), "Integrating optimization and simulation: research and practice", *Simulation Conference Proceedings*, Vol. 1, Winter, pp. 610-6.
- Goldberg, D. (1989), *Genetic Algorithms in Search, Optimization and Machine Learning*, Addison-Wesley Publishing Company, Reading, MA.
- Hashiyama, T., Behrendt, S., Furuhashi, T. and Uchikawa, Y. (1995), "Fuzzy controllers for semiactive suspension system generated through genetic algorithms", paper presented at Intelligent Systems for the 21st Century. IEEE International Conference on Systems, Man and Cybernetics, Vol. 5, pp. 4361-6.
- Herrera, F., Lozano, M. and Sanchez, A.M. (2003), "A taxonomy for the crossover operator for real-coded genetic algorithms: an experimental study", *International Journal of Intelligent Systems*, Vol. 18, pp. 309-38.
- Hounsell, B. and Arslan, T. (2000), "A novel genetic algorithm for the automated design of performance driven digital circuits", *Proceedings of the 2000 Congress on Evolutionary Computation*, Vol. 1, pp. 601-8.
- Kuo, Y.-P. and Li, T.-S. (1999), "Ga-based fuzzy P/PI controller for automotive active suspension system", *IEEE Transactions on Industrial Electronics*, Vol. 46 No. 6, pp. 1051-6.
- Mentor Graphics Corporation (2004), *SystemVision User's Manual*, Version 3.2, Release 2004.3.
- Mitchell, M. (1996), *An Introduction to Genetic Algorithms*, The MIT Press, Cambridge, MA.
- Moon, S.Y. and Kwon, W.H. (1996), "Genetic-based fuzzy control for automotive active suspensions", *Simulation Conference Proceedings*, Vol. 2, pp. 923-9.
- Moser, E. and Mittwollen, N. (1998), "VHDL-AMS: the missing link in system design. Experiments with unified modelling in automotive engineering", *Proceedings on Design, Automation and Test in Europe*, pp. 59-63.
- Rajamani, R. and Hedrick, J. (1994), "Performance of active automotive suspensions with hydraulic actuators: theory and experiment", *Proceedings on American Control Conference*, pp. 1214-8.

- Sam, Y., Ghani, M. and Ahmad, N. (2000), "LQR controller for active car suspension", *Proceedings on TENCON 2000*, pp. 441-4.
- Son, S.-I. and Isik, C. (1996), "Fuzzy control of an automotive active suspension", paper presented at Biennial Conference of the North American Fuzzy Information Processing Society, pp. 377-81.
- Sugeno, M. (1985), "An introductory survey of fuzzy control", *Information Sciences*, Vol. 36, pp. 59-83.
- Tan, H.-S. and Bradshaw, T. (1997), "Model identification of an automotive hydraulic active suspension system", *Proceedings on American Control Conference*, pp. 2920-4.
- Truscott, A. and Burton, A. (1994), "On the analysis, modelling and control of an advanced automotive suspension system", paper presented at International Conference on Control'94, Vol. 1, pp. 183-9.
- Ulsoy, A., Hrovat, D. and Tseng, T. (1994), "Stability robustness of LQ and LQG active suspension", *Journal of Dynamic Systems, Measurement, and Control Transactions of ASME*, Vol. 116, pp. 123-31.
- VDA/FAT Working Group AK 30 (2004), "Guidelines for the development of a VHDL-AMS model library", available at: [www.eas.iis.fraunhofer.de/workgroups/vhdlams/pd/modeling/guidelines\\_ak30.pdf](http://www.eas.iis.fraunhofer.de/workgroups/vhdlams/pd/modeling/guidelines_ak30.pdf)
- Yagiz, N., Ozbulur, V., Inanc, N. and Derdiyok, A. (1997), "Sliding modes control of active suspensions", *Proceedings of the 1997 IEEE International Symposium on Intelligent Control*, pp. 349-53.
- Zadeh, L. (1965), "Fuzzy sets", *Information and Control*, Vol. 8, pp. 338-53.

#### About the authors



L. Wang received his BE degree from Beijing University of Posts and Telecommunications and MSc degree from the University of Liverpool, in 2003 and 2004, respectively. He is currently a postgraduate research student at University of Southampton. His research interests focus on VHDL-AMS based modelling and simulation of mixed physical-domain systems for automotive and MEMS applications. L. Wang is the corresponding author and can be contacted at: [lw04r@ecs.soton.ac.uk](mailto:lw04r@ecs.soton.ac.uk)



T.J. Kazmierski has received a Master of Electronic Engineering Degree from Warsaw University of Technology in 1973 and a PhD degree from the Military Academy of Technology in Warsaw in 1976. He is currently a member of the Electronic Systems Design Group at the School of Electronics and Computer Science. His research interests include numerical modelling, simulation and synthesis techniques for computer-aided design of VLSI circuits. He has published over 100 research papers in this area and in recent years he has been working on applications of hardware description languages to high-level system modelling and synthesis, involving modelling of mixed-domain systems, automated analogue and mixed-signal synthesis for ASIC design, including synthesis of artificial, VLSI neural networks.